Effects of fast mold temperature evolution on micro features replication quality during injection molding

Liparoti, S.; Calaon, M.; Speranza, V.; Tosello, G.; Pantani, R.; Hansen, N. H.; Titomanlio, G.

Published in:
AIP Conference Proceedings

Link to article, DOI:
10.1063/1.5016772

Publication date:
2017

Document Version
Publisher's PDF, also known as Version of record

Effects of Fast Mold Temperature Evolution on Micro Features Replication Quality during Injection Molding

S. Liparoti[a], M. Calaon[b], V. Speranza[a], G. Tosello[b], R. Pantani[a], N.H. Hansen[b], and G. Titomanlio[a*]

[a]*Department of Industrial Engineering, University of Salerno, Italy*
[b]*Department of Mechanical Engineering, Technical University of Denmark, Lyngby, Denmark*

**gtitomanlio@unisa.it*

Abstract

The growing demand to manufacture, with high accuracy, functional structures in the micro and sub-micrometer range polymer based microsystem products calls for reliable mass production processes. Being injection molding (IM) the preferential technology employed for polymer mass fabrication and mold temperature one of the most relevant process parameter to enhance polymer replication at the micro meter scale, the present study investigates effects of fast mold temperature evolution on final replication quality of produced injection molded parts. Micro features master geometries were produced by UV lithography and subsequent nickel electroplating. The mold temperature was controlled by a thin heating device (composed by polyimide as insulating layer and polyimide carbon black loaded as electrical conductive layer) able to increase the temperature on mold surface in a few seconds (40°C/s) by Joule effect and let the surface to cool down soon after. This heating device allowed to maintain mold temperature at a constant value for a time that could be equal to the filling time or longer. A fully characterized isotactic polypropylene was used as the polymer material during the injection molding experiments. The experiments revealed that the replication was mostly sensitive to cavity pressure and mold temperature. In particular, an increase of holding pressure and mold temperature enhanced the replication. Also, the heating time increased the replication quality.

INTRODUCTION

In the last decade a growing interest is focused on microfluidic devices, systems that process or manipulate small (10^{-9} to 10^{-18} litres) amounts of fluids, using channels with dimensions of tens to hundreds of micrometers, thanks to their wide range of possible application in molecular analysis, bio-defence, molecular biology and microelectronics [1]. Despite many advantages presented by microfluidics, the difficulties in mass production have limited their use. Recently, many author proposed to apply UV lithography, nano imprint lithography and e-beam lithography, techniques to produce micro-features on metallic inserts, to injection molding and micro injection molding to obtain high accurate objects for microfluidic devices [2]. Efforts have been devoted to correlate the process parameters of injection molding to replication accuracy [3][4]. One of the most important parameters in controlling replication accuracy seems to be mold temperature [5][6], however, the increase of mold temperature is generally not preferable since it requires additional cycle time. For this reason, many attempts to fast control mold temperature have been reported in the literature. Induction coils [7], radiation [6] or proximity heating [8] have been proposed to increase mold temperature on the cavity surface. However, these technologies suffer of some limitations, as high additional design and tool costs and small temperature increase/decrease velocity that make too long the cycle time. As far as cycle time is concern, a different approach has been proposed in [9] to overcome this issue. The design made of two insulation layers with a resistance layer in between allows for fast and effective heating phase reducing so cycle time compared with other studies [10–12].

In this paper, a conductive polymeric film, composed by poly(imide-amide) loaded carbon black, have been used to fast control mold surface temperature. This heating device allows to maintain mold temperature at a constant value for a time that could be equal to the filling time or longer, and the reduced thickness allows a fast cooling after heater deactivation. Main focus of the paper is given on the equipment capability of enhancing polymer replication fidelity for produced µm test structures on a nickel shim. Structures widths at different process settings have been quantified. Selected samples have been qualitatively analyzed to study effects of temperature evolution and its effect on molded microstructures morphologies.

EXPERIMENTAL

Molding experiments were carried out using polypropylene (i-PP) grade supplied by Montell (now Basell), with commercial name T30G (non-nucleated, Mw=376 000, Mw/Mn=6.7, tacticity=87.6%). A conductive polymeric film, polyimide loaded carbon black (ENSACO 260G, 30% w), with thickness of 50 µm and 40 Ω/square as sheet resistance [13], is layered between two insulating layers of polyimide and applied on both sides of the cavity, giving rise to the

Proceedings of PPS-32
AIP Conf. Proc. 1914, 140007-1–140007-5; https://doi.org/10.1063/1.5016772
Published by AIP Publishing. 978-0-7354-1606-2/$30.00

mold surface heating. The nickel shim whose surface contains the micro-crosses to replicate in the moldings is located on the heater.

The master geometries were originally fabricated using a 365 nm UV mask aligner process with 2 mask layers on a 100 mm silicon wafer. Both layers were defined in AZ5214E photoresist layer and dry etched using a reactive ion etching (RIE), which produced the final structures depth in the silicon substrate. After structure fabrication into the silicon sacrificial layer a titanium/ nickel seed layer with a thickness of 10 nm and 100 nm respectively, was deposited by sputter deposition prior to electroplating of a 320 µm nickel layer. Wire electrical discharge machining was finally employed to cut the nickel shim, later used during the experimental phase, with required dimension to fit the mold design and structure.

A 70-ton Negri-Bossi reciprocating screw, injection molding machine was used for the experiments. The polymer was injected into line-gated rectangular cavities having length L=107 mm, width W=12.7 mm, and thicknesses S=1.5 mm. Fig 1 shows the cavity used for the injection experiments, a sketch of the heater is also reported. The heater has a length of 70 mm. The nickel insert, 19x19 mm2, is located downstream the gate. Where the nickel insert is not present a steel layer of the same thickness is located. The molding machine and the mold were equipped with five piezoelectric transducers: one in the injection chamber (P0), one just before the gate (P1) and three in the cavity (P2, P3 and P4), located in the non-moving part of the mold (15, 60 and 105 mm downstream from the gate position). Moreover, a temperature sensor was located in the cavity, on the steel layer, in positions P2.

All the experiments were carried out keeping constant the flow rate at 2.8 cm^3/s, the holding time at 8s, the melt temperature at 220°C, and the mold temperature, except on the heated surface, at 28°C. Experiments were carried out supplying two electrical power densities, 7 and 10 W/cm^2, to the heating device, for different times (t_h), 1.3s, 8s and 13s. TABLE 1 summarizes the experimental conditions.

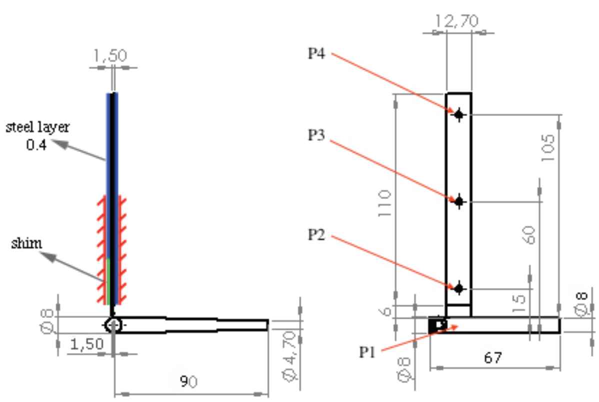

FIGURE 1 Geometry of the cavity (P1-P4 indicate the pressure transducers positions) and sketch of the heating device.

Test run	*P* *(W/cm^2)*	*T_{level} (°C)*	*t_h (s)*	*t_a (s)*	*P_{hold}*
p-passive*l*	0	28	0	0	360
p-passive*h*	0	28	0	0	720
p-1201*h*	7	120	1.3	4	720
p-12013*h*	7	120	13	4	720
p-1501*h*	10	150	1.3	4	720
p-1501*l*	10	150	1.3	4	360
p-1508*h*	10	150	8	4	720
p-15013*h*	10	150	13	4	720
p-15013*l*	10	150	13	4	360

TABLE 1 Operating conditions adopted for the injection molding experiments. (P=electrical power applied; T_{level}= temperature reached on the steel layer; t_h=time that the heater is activated after the polymer reaches position P2. t_a = time that the heater was activated before the contact with the polymer in P2: P_{hold}=holding pressure).

FIGURE 2 shows the pressure evolution at the five transducer positions related to the experiments p-passiveh, performed without activating the heater (FIGURE 2a), and activating the heater for 13s with a power density of 10 W/cm2 (FIGURE2b).

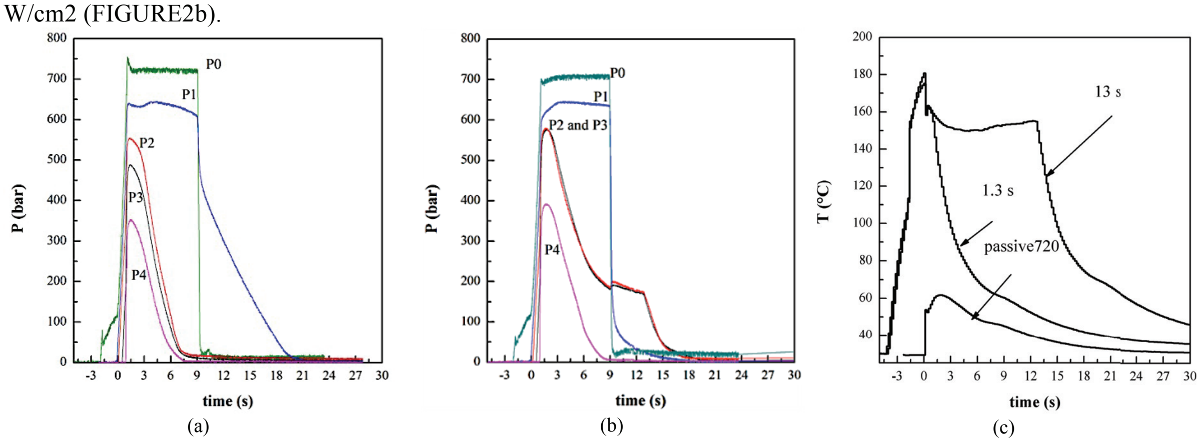

FIGURE 2 Pressures in different transducer positions, related to the experiment (a) p-passive*h* and (b) p-15013*h*. (c) Temperature evolutions related to the experiments p-1501*h*, p-15013*h* and for p-passive*h*.

The gate sealing takes place at t=3.5s in both cases. However, when the heater is active pressures in positions P2 and P3 go to zero into two steps, the first one due to the decrease of the average temperature from the melt temperature to the surface temperature, 150°C in this case, and the second, that takes place at the heater deactivation, from 150°C to the selected mold temperature. Also pressure in position P4 goes to zero with a certain delay, about 1.3s, with respect to pressure decay at the same position for the experiment p-passiveh. Similar pressure evolutions have been obtained supplying a lower electrical power density, 7 W/cm^2, to the heater.

FIGURE 2c shows temperature evolutions in position P2 for the three experiments p-passiveh, p1501h and p15013h. The heater is activated 4s before the melt reaches position P2 (t=0), during such a time temperature on the surface goes from the mold temperature to 150°C. The temperature increase during the range -1.5s<t<0s is due to the decrease of the contact resistance and the consequent current increase. When the polymer reaches position P2, the temperature reaches the maximum value and soon after it starts to decrease to the selected surface temperature.

RESULTS AND DISCUSSION

To analyze the effect of the process conditions on the replicability, micro-crosses, detected on the sample surface, have been observed by Atomic Force Microscope (AFM) in tapping mode (commercial probe tips with nominal spring constants of 42 N m^{-1}, resonance frequencies of 300 kHz, and tip radius of 7 nm have been used). **FIGURE 3** shows the AFM height images of micro-crosses, 20 μm wide, on the nickel insert and of micro-crosses replicated on the samples p-passiveh and p15013h.

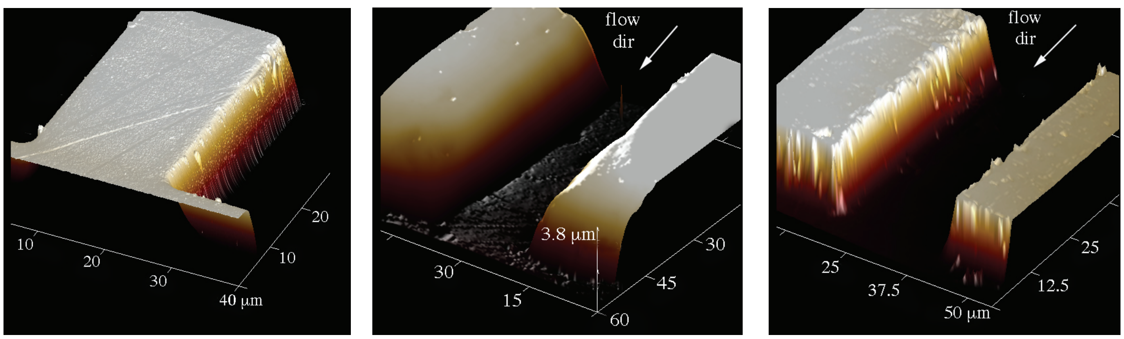

nickel insert passive720 150°C 13s 720bar

FIGURE 3 AFM height images of the micro-crosses having a width of 20 μm on the nickel insert and of micro-crosses replicated on the samples p-passive*h* and p-15013*h*. The flow direction is also indicated.

The AFM height images show that mold surface temperature is a very important parameter in achieving good microstructure replication. Indeed, the micro-cross replicated on p-15013h sample appears to have a sharper edge than the micro-cross in p-passiveh sample, and this can be seen especially at the corners.

To quantify the accuracy of the micro-crosses replication the traces and retraces (at 20 μm from the corner), obtained by AFM analysis, have been analyzed considering errors due to the interaction between the sample and the tip [14]. In particular, the absolute values of the trace derivative have been fitted by an asymmetric double sigmoidal function, and the full with at half maximum (H_f) has been chosen as accuracy index. A micro feature having a sharp edge shows a small H_f, close to the value of the shim (2.2±0.8μm). The height of the micro-cross is 5±0.2 μm for all the samples, for this reason as output analysis to establish the replication fidelity as a function of different process parameters the width of the replicated structures was quantified. **FIGURE 4** shows the AFM height trace, the absolute value of the derivate and the fitting curves obtained for the micro-cross located on the nickel insert and for the micro-cross replicated on the sample p-15013h.

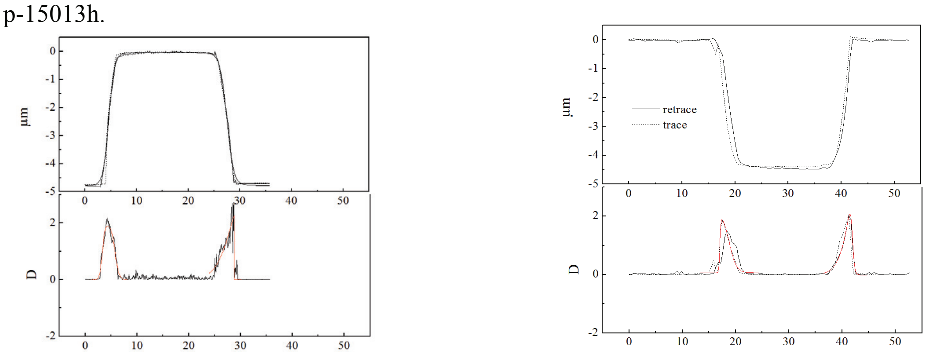

(a) (b)

FIGURE 4 Profile of the micro-cross on the shim (a) and on the sample p-15013*h* (b). The absolute value of the profile derivative and their fitting by asymmetric double sigmoidal function are also reported.

FIGURE 5 shows the comparison of the H_f obtained fitting the trace/retrace of AFM height data obtained for samples produced in different packing conditions and supplying 7 and 10 W/cm^2 to the heating device. Data have been sorted on the bases of the AFM analyzed position on the micro-crosses as reported in **FIGURE 5c**.

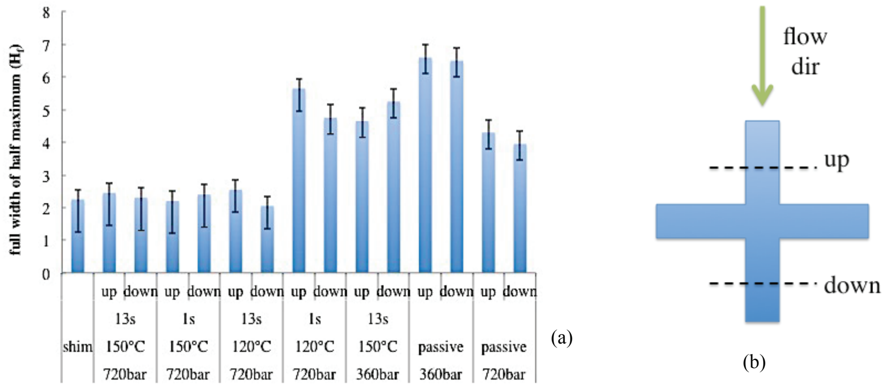

FIGURE 5 Comparison of the H_f evaluated for samples produced in different injection molding conditions. (a) Branch parallel to the flow direction. (b) Sketch of the analyzed positions on the micro-crosses. Error bars indicate the deviation from the real value due to the interaction between the tip and the sample.

The comparison between p-passivel and p-passiveh suggests that packing pressure has a significant effect on the replicability: the replication is improved by selecting higher packing pressure, however, the H_f calculated for p-passiveh sample is still larger than the value calculated for the nickel insert. Only selecting higher temperatures (120°C and 150C°) the H_f becomes closer to the value of the nickel insert. **FIGURE 6a** shows that H_f is small for all the samples produced selecting 150°C as mold surface temperature at all the considered heating times, whereas, decreasing mold surface temperature to 120°C the replication becomes poor at small heating time (1.3s). This behavior can be explained considering that during the time in which the heater is active higher pressures can be applied for longer time (see **FIGURE 2**), and this results in a better replication. When 150°C is selected as mold surface temperature this effect is less significant because a better replication is already achieved during the filling stage.

The mold surface temperature evolution has a significant effect on the morphology of the molded samples [10,12]. For this reason a qualitative investigation on the molded microstructure morphology has been performed. Slices, cut perpendicular to the flow direction in position P2, where the micro-crosses are also located, have been observed by optical microscope, with crossed analyzer and polarizer. **FIGURE 6** shows optical micrographs related to the molded samples p-passivel, p-passiveh, p15013l and p15013h.

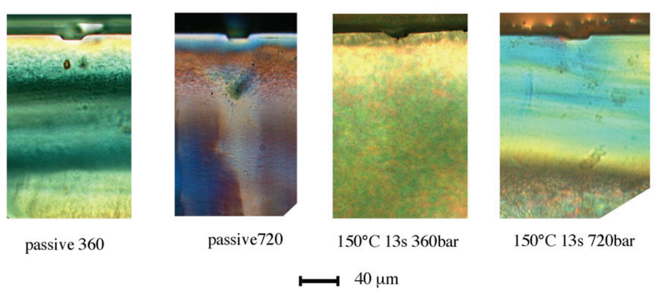

FIGURE 6 Optical micrographs of the slices cut from the samples p-passive360, p-passive720, p-15013*l* and p-15013*h,* near the micro-crosses having a width of 20 μm. Flow direction at 45° respect to polarizer direction.

As observed in other works [15–21], the skin layer is drastically reduced when the mold temperature is kept high during the injection molding process; the shear layer, that is also reduced by the use of higher mold temperature, disappears when the lower packing pressure is selected, in this case only spherulitical structures can be observed. These phenomena can be explained taking into account the relaxation of the molecular stretch and orientation that take place at higher temperature [10]. Preliminary conclusions from the qualitative investigation (FIGURE 6) indicate no visible effect on the structures morphology.

CONCLUSIONS

In this work, injection molding coupled with fast control of mold surface temperature have been proposed for the mass production of samples with micro-features, since the heating device is able to produce fast temperature evolution giving rise only a reduced cycle time increase. A nickel insert, having microstructures produced by UV lithography, has been located on the mold surface, where the heating device was present.

Packing pressure increase has been found to improve micro-crosses replication. However, additional packing pressure is not sufficient to achieve high accurate replication. Mold surface temperature is the most important parameter in controlling replication of microstructures, since mold surface temperature of 150°C allows to produce samples with microstructures very similar to those located on the master geometry. The presence of micro-crosses on the nickel insert does not seem to influence the morphology of the molded samples.

REFERENCES

1 G.M. Whitesides, Nature. 442 368–373 (2006). http://dx.doi.org/10.1038/nature05058.

2 S. Menotti, H.N. Hansen, G. Bissacco, M. Calaon, P.T. Tang, C. Ravn, The International Journal of AdvancedManufacturing Technology. 74 907–916 (2014).

3 H.-L. Lin, C.-S. Chen, R.-T. Lee, S.-C. Chen, R.-D. Chien, M.-C. Jeng, et al., Japanese Journal of AppliedPhysics. 52 44001 (2013). http://stacks.iop.org/1347-4065/52/i=4R/a=044001.

4 M. Calaon, G. Tosello, H.N. Hansen, J. Nő regaard, Influence of process parameters on edge replication quality of lab-on-a-chip micro fluidic systems geometries, in: Annual Technical Conference - ANTEC, Conference Proceedings, 2013: pp. 1084–1088. http://www.scopus.com/inward/record.url?eid=2-s2.0-84903544048&partnerID=tZOtx3y1.

5 S. Liparoti, T.M. Hunag, A. Sorrentino, G. Titomanlio, M. Cakmak, Rapid control of mold temperature during injection molding process, in: 30th International Conference of Polymer Processing Society, Cleveland, Ohio, USA - AIP Conference Proceeding, 2014: p. 110015.

6 S.-C. Chen, Y. Chang, Y.-P. Chang, Y.-C. Chen, C.-Y. Tseng, International Communications in Heat and Mass Transfer. 36 1030–1035 (2009).

7 H.L. Lin, S.C. Chen, M.C. Jeng, P.S. Minh, J.A. Chang, J.R. Hwang, International Communications in Heat and Mass Transfer. 39 514–522 (2012).

8 D. Yao, T.E. Kimerling, B. Kim, Polymer Engineering & Science. 46 938–945 (2006).

9 K.M.B. Jansen, A.A.M. Flaman, Polymer Engineering & Science. 34 894–897 (1994).

10 S. Liparoti, A. Sorrentino, G. Guzman, M. Cakmak, G. Titomanlio, RSC Advances. 5 36434–36448 (2015).

11 S. Liparoti, A. Sorrentino, G. Titomanlio, RSC Advances. 6 99274–99281 (2016).

12 S. Liparoti, A. Sorrentino, G. Titomanlio, AiChE Journal. 62 2699 (2016).

13 S. Liparoti, G. Landi, A. Sorrentino, V. Speranza, M. Cakmak, H.C. Neitzert, Advanced Electronic Materials. 21600126 (2016).

14 G. Tosello, A. Antico, H.N. Hansen, F. Marinello, G. Lucchetta, Influence of measuring parameters on the precision of atomic force microscope in industrial applications, in: International Conferences on Multi-Material Micro Manufacture, 4M/International Conferences on Micro Manufacturing, ICOMM, 2009: pp. 401–406.

15 S. Liparoti, A. Sorrentino, G. Titomanlio, Rapid control of mold temperature during injection molding process: Effect of packing pressure, in: Polymer Processing with Resulting Morphology and Properties: Feet in the Present and Eyes in the Future: Proceedings of the GT70 International Conference - Salerno (Italy) 2015. AIP Conference Proceedings, 2015: p. 20052.

16 S. Liparoti, T.M. Hunag, A. Sorrentino, G. Titomanlio, M. Cakmak, Proceeding of PPS-30: The 30thInternational Conference of the Polymer Processing Society - Cleveland (Ohio US) 2015. AIP Conference Proceedings. 1664 (2015).

17 S. Liparoti, A. Sorrentino, G. Guzman, M. Cakmak, G. Titomanlio, Effect of fast mold surface temperature evolution on iPP part morphology gradients, in: PROCEEDINGS OF PPS-31: The 31st International Conference of the Polymer Processing Society–AIP Conference Proceeding, 2016: p. 170001.

18 R. Pantani, I. Coccorullo, V. Speranza, G. Titomanlio, Progress in Polymer Science. 30 1185–1222 (2005).

19 R. Pantani, F. De Santis, V. Speranza, G. Titomanlio, Modelling morphology evolution during solidification of IPP in processing conditions, AIP Conference Proceedings, 1593, pp. 636-640 (2014).

20 R. Pantani, V. Speranza, G. Titomanlio, Simultaneous morphological and rheological measurements on polypropylene: Effect of crystallinity on viscoelastic parameters, Journal of Rheology. 59 (2) 377-390 (2015).

21 V. Speranza, U. Vietri, R. Pantani, Monitoring of injection molding of thermoplastics: Average solidification pressure as a key parameter for quality control, Macromolecular Research. 19 (6) 542-554 (2011).